Genomic and proteomic characterization of sulfate-reducing symbionts of gutless marine annelids

Grace D'Angelo[1], Manuel Kleiner[2], Anna Mankowski[3], Jerónimo Cifuentes-Anticevic[1], Marlene J. Violette[4], Valerie De Anda[5], Eileen Kröber[1], Nicole Dubilier[1,6*], Manuel Liebeke[1,7*]

[1]Max Planck Institute for Marine Microbiology, Bremen, Germany

[2]Department of Plant and Microbial Biology, North Carolina State University, Raleigh, NC, USA

[3]Structural and Computational Biology Unit, European Molecular Biology Laboratory, Heidelberg, Germany

[4]Department of Biostatistics and Bioinformatics, Duke University School of Medicine, Durham, NC, USA

[5]University of Texas at Austin Marine Science Institute, Austin, TX, USA

[6]MARUM Center for Marine Environmental Sciences, University of Bremen, Bremen, Germany

[7]Institute of Human Nutrition and Food Science, Department of Metabolomics, University of Kiel, Kiel, Germany

*corresponding authors: mliebeke@mpi-bremen.de, ndubilier@mpi-bremen.de

Abstract

Sulfate-reducing bacteria inhabit marine and terrestrial environments, forming syntrophic associations with other bacteria, archaea and eukaryotes. A notable example is the symbiosis between sulfate-reducing bacteria (SRB) and gutless oligochaete worms found in marine sediments worldwide. These endosymbionts participate in a syntrophic sulfur exchange with the primary endosymbiont of gutless oligochaetes, a sulfur-oxidizing bacterium, thus providing otherwise inaccessible metabolic capabilities to the animal host. Here, we used a combination of metagenomic and metaproteomic analysis to describe the metabolic functions of SRBs from gutless annelids. Identified as members of the Desulfobacteria class, closely related to the *Desulfococcus* and *Desulfosarcina* genera, these SRB symbionts exhibit a range of common and unique metabolic capabilities. Our analyses revealed their core metabolism of complete oxidation of acetate to CO_2 via the Wood-Ljungdahl pathway, glyoxylate bypass of the TCA cycle, degradation of glycine as a nitrogen source, and presence of transporters for essential nutrients. A large-scale genome comparison revealed that the sulfate-reducing endosymbionts, named here "*Candidatus* Desulfoconcordia", have metabolic distinctions with respect to their free-living counterparts that could indicate adaptation to the energy and nutrient requirements of their symbiotic niche. The enrichment of functions like peptidases and amino acid transporters together with their abundant expression in the proteomes and the reduction of sugar and sulfur scavenging functions in the symbiotic genomes indicate a symbiosis-driven ecological role distinct from free-living SRBs. Our study revealed the metabolic capabilities that have enabled "*Candidatus* Desulfoconcordia" to adapt to their multi-domain associations.

Introduction

Sulfate-reducing microorganisms (SRM) collectively represent microbes with the capacity for dissimilatory sulfate reduction, whereby sulfate is used as the terminal electron acceptor in the oxidation of organic and inorganic substrates (Postgate, 1979). SRM are found throughout the tree of life and have a wide range of possible substrates, allowing for metabolic versatility and the adaptability to diverse habitats (De Anda et al., 2018). These organisms have been described in sewage, aquatic microbial communities, deep-subsurface sediments, and animal microbiomes (Barton & Fauque, 2022; De Anda et al., 2018; Diao et al., 2023; Hao et al., 1996; Kushkevych et al., 2020; Langwig et al., 2022). The symbiotic consortia of marine gutless annelids is one such example of an animal microbiome that includes sulfate-reducing bacteria. (Dubilier et al., 2001; Ruehland et al., 2008; Woyke et al., 2006).

This symbiotic consortium is defined by the association with a primary thioautotrophic endosymbiont (Dubilier et al., 2001) and the co-occurrence of secondary endosymbionts – including alphaproteobacteria, Desulfobacteria, and spirochetes – the specific composition of which varies with host species and location (Mankowski et al., 2021; Ruehland et al., 2008; Woyke et al., 2006). All gutless oligochaete host species exist in an obligatory nutritional symbiosis driven by the chemosynthetic metabolism of their primary symbiont, *Candidatus* Thiosymbion (Bergin et al., 2018; Dubilier et al., 2001; Ruehland et al., 2008; Zimmermann et al., 2016). This primary chemoautotrophic symbiont uses sulfide as an electron donor to fix inorganic carbon using Type 1 RuBisCo in the Calvin-Benson-Bassham (CBB) cycle (Dubilier et al., 2001). *Ca.* Thiosymbion build up large amounts of carbon storage compounds, making their digestion a key component of nutrition for the host cells (Kleiner et al., 2023). This interplay between the chemoautotrophic symbionts and the gutless marine worm has been studied in detail (Dubilier et al., 2001; Kleiner et al., 2012, 2015; Woyke et al., 2006); what complicates our understanding of this consortia is the diverse and variable associations of these

65 animals with secondary sulfate-reducing bacterial (SRB) symbionts. Secondary sulfate-
66 reducing endosymbionts, which occur in multiple host species worldwide, are known to recycle
67 waste products that host cells are otherwise unable to utilize. This has been previously
68 demonstrated by the observation that high-affinity uptake transporters make up ca. 38% of the
69 proteome in the SRB symbionts of one host species, *Olavius algarvensis* (Kleiner et al., 2012).
70 The expression of ABC and TRAP-type transporters for substrates, including amino acids,
71 peptides, carboxylates, sugars, polyamines, and phosphonates, suggests that these heterotrophs
72 depend on organic substrates as both energy sources and building blocks in central metabolism.

73 Previous studies of the gutless oligochaete host, *Olavius algarvensis*, have described a
74 consortium comprising two sulfur-oxidizing symbionts (*Ca.* Thiosymbion and another
75 gammaproteobacterium 'Gamma 3'), multiple sulfate-reducing symbionts (Delta 1, Delta 3,
76 and Delta 4), and spirochetes (Dubilier et al., 2001; Kleiner et al., 2012; Ruehland et al., 2008;
77 Sato et al., 2022; Woyke et al., 2006). According to the study on a single host species, SRB
78 symbionts made up approximately 15% of the relative read abundance in the metagenomes
79 (Sato et al., 2022). A recent study encompassing sampling sites around the world, revealed
80 diverse patterns of symbiotic associations, including the different combinations and
81 abundances of co-occurring symbionts in individual specimens of multiple host species
82 (Mankowski et al., 2021). To increase our understanding of the metabolic niches these
83 organisms fill, we describe a clade of symbiotic sulfate-reducing bacteria that associate with at
84 least 14 species of gutless oligochaete hosts. We focused on profiling and understanding the
85 metabolic predictions and expressed physiology of one abundant sulfate-reducing symbiont
86 clade in gutless oligochaetes, previously referred to as Delta 4 (Mankowski et al., 2021). We
87 aimed to expand our understanding of their nutritional role in their association with a host, their
88 involvement in a syntrophic microbial community with a reduced and defined complexity, and
89 their possible role in the geochemical sulfur and carbon cycles in coastal marine sediments.

90 Due to the nature of the mutually beneficial role they play in this symbiotic association, we
91 propose the novel genus name "*Candidatus* Desulfoconcordia." [L. fem. n. *concordia,* union,
92 concurrence, harmony]. In this study, we used a combined metagenomic, metatranscriptomic,
93 and metaproteomic approach to understand the phylogeny, classify the metabolic capabilities,
94 and establish the role of endosymbiotic "*Ca.* Desulfoconcordia".

95 Results

96 *"Ca.* Desulfoconcordia" form a distinct symbiotic clade in the class of Desulfobacteria

97 Recently published metagenome assembled genomes of the deltaproteobacterial symbionts
98 from gutless oligochaetes, from now on "*Ca.* Desulfoconcordia" symbionts, were used
99 alongside publicly available genomes, to investigate the genomic potential of these symbiotic
100 sulfate-reducers (Mankowski et al., 2021). Metagenome assembled genome bins were selected
101 based on completeness and contamination values reported by CheckM. All bins were over 80%
102 complete and less than 10% contaminated. All 45 genomes used in this study had at least one
103 rRNA operon and at least 18 unique tRNAs represented (A full summary of the genome
104 features can be found in **Table S1**). The symbiont bins were assembled previously from
105 metagenomes generated from sequencing multiple host species collected in various coastal
106 habitats around the world including Hawai'i, Australia, Italy, Belize, and the Bahamas
107 (Mankowski et al., 2021; **Table S1**). To cover many habitats, host animals were collected from
108 sediments around seagrass meadows and coral reefs with a few collected from locations with
109 only sandy or muddy sediment (**Table S1**).

110 We constructed a phylogenomic tree based on a hidden Markov model (HMM) database of 74
111 bacterial single-copy genes to place the "*Ca*. Desulfoconcordia" metagenome-assembled
112 genomes (MAGs) in context with all Desulfobacteria entries from the Genome Taxonomy
113 Database.

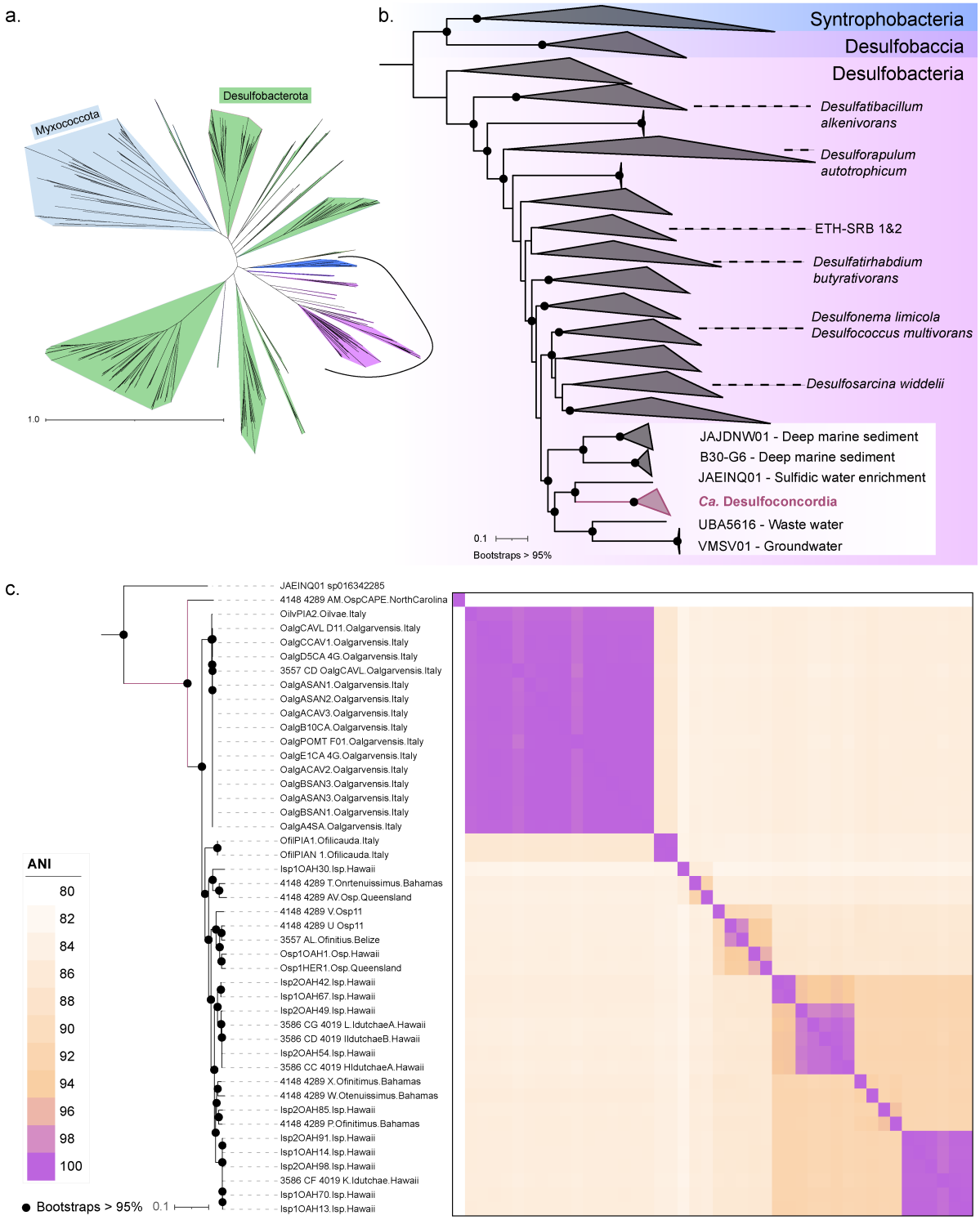

Figure 1: Phylogenomic placement of "*Ca.* Desulfoconcordia" symbionts. The "*Ca.* Desulfoconcordia" symbiont metagenome-assembled genome bins are displayed in their phylogenomic context according to the GToTree workflow for GTDB reference genomes. a) Phylogenomic tree generated with 426 publicly available genomes and 14 metagenome-assembled genome bins of "*Ca.* Desulfoconcordia" symbiont places these symbionts in the Desulfobacteria class (**Table S8**). b) For a more detailed view, the classes Syntrophobacteria and Desulfobaccia were used as outgroups for the class Desulfobacteria. Selected representative type strain members of Desulfobacteria are highlighted in their respective clades. Close representatives to the monophyletic "*Ca.* Desulfoconcordia" symbiont clade are labeled with their GTDB taxonomic genus-level identifiers. Black dots represent UltraFast bootstrap scores greater than 95%.

124 The symbiont MAGs formed a clade that was sister to the GTDB-classified organism
125 JAEINQ01 (**Fig. 1**), a genome assembled from a cellulose-fed sulfidic water enrichment
126 originating from the Black Sea (NCBI GCA_016342285.1). Other close relatives included
127 uncultivated organisms from marine sediments next to hydrothermal vents, groundwater, and
128 wastewater (**Fig. 1b**). These uncultivated relatives also included GTDB genus-level classified
129 genomes from more than one environment. Genomes belonging to the genus B30-G6 come
130 from both marine (Dombrowski et al., 2018) and river sediments (Tee et al., 2021), whereas
131 the genus JAJDNW01 is primarily described from hydrothermal vent sediment (Langwig et
132 al., 2022). One member of this genus was isolated from the rhizosphere of salt marsh grass
133 (NCBI GCA_022340465.1). The closest related cultivars, which included the genera
134 *Desulfonema, Desulfococcus,* and *Desulfosarcina,* were within the nearest sister clade (**Fig.**
135 **1b**).

136 The "*Ca.* Desulfoconcordia" genomes formed a monophyletic clade, demonstrating a cohesive
137 genetic lineage despite their worldwide sampling locations. These symbiont genomes were
138 associated with two host genera comprising 14 host species sampled across multiple years and
139 diverse habitats (**Table S1**). Average nucleotide identity (ANI) analysis (**Fig. 1c**) showed that
140 "*Ca.* Desulfoconcordia" symbionts represent diversity below the typical species-level
141 threshold of 95% (Goris et al. 2007) ANI. Most genomes ranged between 82 – 100% ANI with
142 one another. Genomes that were most similar to one another occur in the same or sympatric
143 host species. For example, "*Ca.* Desulfoconcordia" symbionts of the two *Olavius* host-species
144 that co-occur on the island of Elba in the Mediterranean (Giere & Erséus, 2002) shared over
145 95% ANI similarity with one another (**Fig 1c**). Conversely, a "*Ca.* Desulfoconcordia" genome
146 obtained in North Carolina, USA, is still a member of the monophyletic clade but shares less
147 than 80% ANI with all other members of the clade, representing a more diverged member of
148 the genus (**Fig. 1c**).

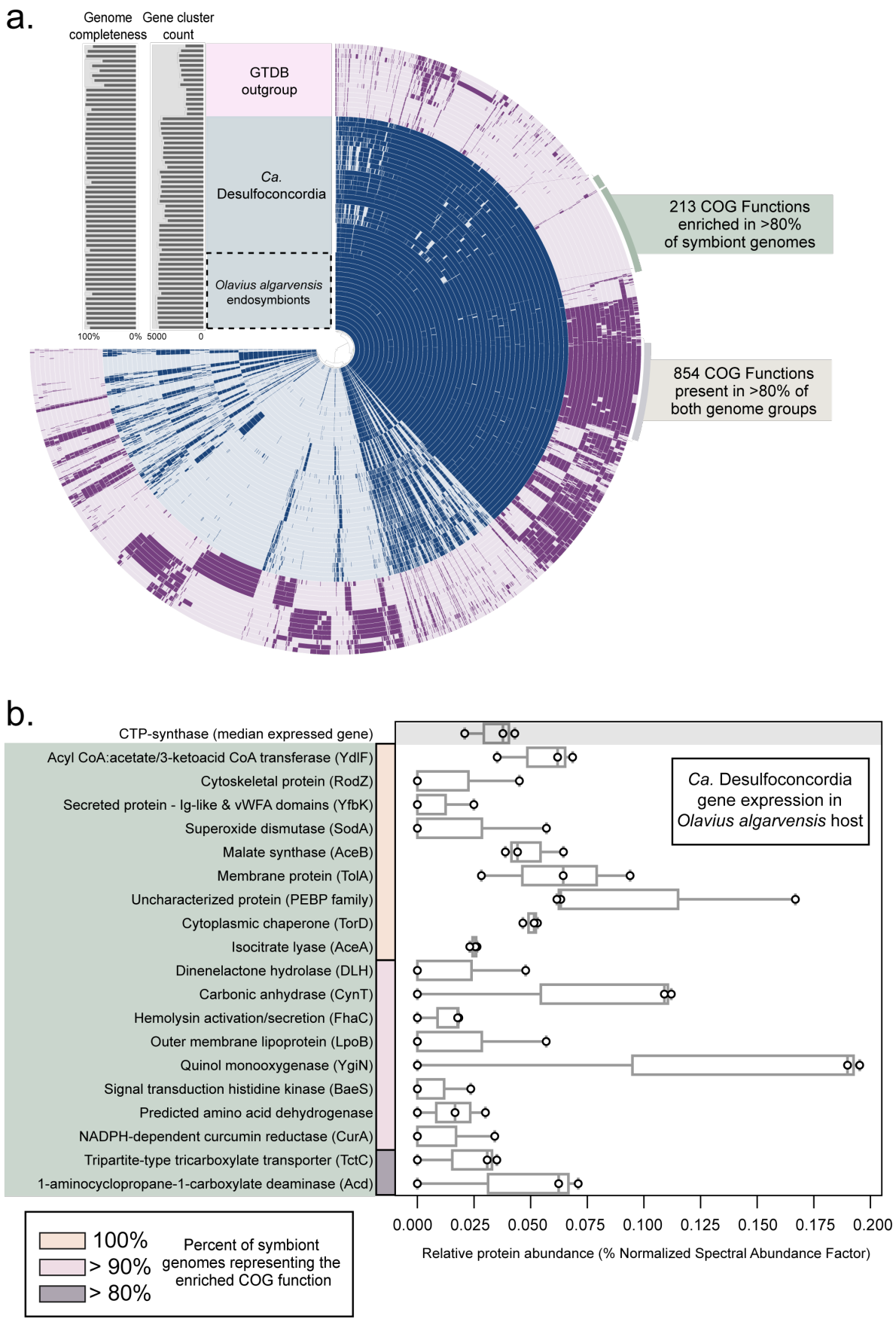
a.
Genome completeness
Gene cluster count
GTDB outgroup
Ca. Desulfoconcordia
Olavius algarvensis endosymbionts
100%
0%
5000
0
213 COG Functions enriched in >80% of symbiont genomes
854 COG Functions present in >80% of both genome groups
b.
CTP-synthase (median expressed gene)
Acyl CoA:acetate/3-ketoacid CoA transferase (YdlF)
Cytoskeletal protein (RodZ)
Secreted protein - Ig-like & vWFA domains (YfbK)
Superoxide dismutase (SodA)
Malate synthase (AceB)
Membrane protein (TolA)
Uncharacterized protein (PEBP family)
Cytoplasmic chaperone (TorD)
Isocitrate lyase (AceA)
Dinenelactone hydrolase (DLH)
Carbonic anhydrase (CynT)
Hemolysin activation/secretion (FhaC)
Outer membrane lipoprotein (LpoB)
Quinol monooxygenase (YgiN)
Signal transduction histidine kinase (BaeS)
Predicted amino acid dehydrogenase
NADPH-dependent curcumin reductase (CurA)
Tripartite-type tricarboxylate transporter (TctC)
1-aminocyclopropane-1-carboxylate deaminase (Acd)
Ca. Desulfoconcordia gene expression in Olavius algarvensis host
0.000
0.025
0.050
0.075
0.100
0.125
0.150
0.175
0.200
Relative protein abundance (% Normalized Spectral Abundance Factor)
100%
> 90%
> 80%
Percent of symbiont genomes representing the enriched COG function

150 **Figure 2: Enriched symbiont gene clusters exhibit expression levels higher than the median in**
151 **"*Ca.* Desulfoconcordia" metaproteomes** a) Functional enrichment analysis of symbiont genomes and
152 close relatives in the GTDB revealed 213 COG20 annotated gene clusters that were present in at least
153 80% of the symbiont genomes and in 0% of the GTDB outgroup. b) Functionally enriched gene clusters
154 are expressed (19/213) in the host species *Olavius algarvensis* Metaproteomic data from enrichments
155 (50 worms homogenized per sample, n=3). Relative protein abundance is presented as percent
156 normalized spectral abundance factor (%NSAF).

157 **Multiple gene enrichment analyses reveal the symbiont-specific functional potential**
158 **of "*Ca.* Desulfoconcordia"**

159 To explore how the members of the symbiont clade compare to their closest phylogenetic
160 relatives, we performed multiple comparative pangenome analyses – one comparison against
161 the uncultivated GTDB relatives (**Fig. 2a**) and one against selected cultivated and syntrophic
162 representatives from the Desulfobacteria class (**Fig. S2**). In both comparisons, the symbiont
163 genomes were generally 0.5 – 1.5 Mbps larger than their free-living counterparts (average size
164 ca. 5 Mbp, **Table S1**), and consequently, they contained more functionally annotated genes.
165 (**Fig. 2a**).

166 A KEGG-module-based metabolic enrichment analysis performed on the core and pangenomes
167 of the symbiont clade and their closed free-living relatives **(Fig. 2a**) revealed that the metabolic
168 modules for the glyoxylate cycle, menaquinone biosynthesis, and pentose phosphate pathway
169 were complete in more than 75% of the symbiont genomes and absent from the free-living
170 genomes. Conversely, fatty acid, thiamine, and polyamine biosynthesis were present in a
171 fraction of the free-living genomes and absent in the symbiont genomes (**Table S2**). A few
172 examples of specific enriched genes in the symbiont group (present in 100% of the symbiont
173 genomes and absent in 100% of the genomes of free-living relatives) include a Zn-dependent
174 protease (YugP), benzoyl-CoA reductase, flagella synthesis proteins, a rhodanese-related
175 sulfurtransferase, and amino acid transporters (e.g. ArgO and PutP). The genomes of the free-
176 living relatives were enriched in the TauABCD system responsible for sulfonate transport
177 (**Table S3**).

178 Functional enrichment analysis of symbiont "*Ca.* Desulfoconcordia" genomes and the GTDB
179 environmental Desulfobacteria outgroup (**Fig. 1b**) revealed 213 gene clusters that were
180 enriched in at least 80% of the symbiont genomes and absent in all the GTDB outgroup
181 genomes (83 of the 213 clusters were present in 100% of the symbiont genomes).

182 **Proteomics revealed expression of symbiont-enriched functions in a lineage of "*Ca.***
183 **Desulfoconcordia" from a Mediterranean host species**

184 To complement this functional enrichment analysis, we used the functionally enriched gene
185 clusters and their assigned Database of Clusters of Orthologous Genes (COG20) Functions (for
186 the full list, see **Table S3**) to determine which of these proteins were present in symbiont-
187 enriched metaproteomes from one Mediterranean host species, *Olavius algarvensis*. To
188 generate these metaproteomes, we homogenized 50 individual host animals and separated the
189 host cells, large bacterial cells, and small bacterial cells by density centrifugation, extracted
190 proteins, and measured them using mass spectrometry. Of the 213 symbiont-enriched COG
191 functions, 19 were detected in the metaproteome within the range or at a slightly higher relative
192 protein abundance than from a median-expressed gene (CTP-synthase) (**Fig. 2**). These data
193 together demonstrated that the symbionts differ from their close relatives in their functional
194 potential. Our metaproteomic evidence shows that "*Ca.* Desulfoconcordia" associated with the
195 host *Olavius algarvensis* were actively translating these symbiont-specific genes in their
196 environment.

197 Filtering the metaproteome results by symbiont-enriched gene clusters allowed us to focus on
198 a set of genes that may be more relevant to the symbiotic lifestyle of these bacteria with respect
199 to free-living relatives. By combining the predicted functions of the "*Ca*. Desulfoconcordia"
200 symbionts with the expression analysis we found that acetate metabolism, cellular
201 maintenance, cell-cell interaction mechanisms, and some uncharacterized functions were
202 enriched and expressed by these bacteria *in situ* (**Fig. 2b**). Isocitrate lyase (AceA) and malate

203 synthase (AceB), which are the two major enzymes used in the glyoxylate bypass of the TCA
204 cycle, were present in a similar relative abundance to the median expressed gene (CTP-
205 synthase). The cytoskeletal protein RodZ, superoxide dismutase, and carbonic anhydrase,
206 which maintain cellular integrity, were detected in at least one of the enrichment samples.
207 Proteins with secreted Ig-like domains and hemolysin secretion for potential interactions with
208 neighboring bacteria or host cells were also detected in the proteome. One gene that was
209 annotated by COG20 functional assignment as either catechol 2,3-dioxygenase for the
210 degradation of aromatic compounds or a quinol monooxygenase involved in general electron
211 transporter maintenance was detected in relatively high abundance in two samples. Finally, one
212 uncharacterized conserved protein that may belong to the phosphatidylethanolamine-binding
213 protein (PEBP) family was present in all three metaproteomes at a relative protein abundance
214 higher than the median expressed gene (**Fig. 2b**). Of the 213 functions that were enriched
215 according to the Anvi'o analysis, 19 functions were covered by expressed proteins under
216 environmental conditions. This filtering method enabled us to pinpoint key metabolic
217 predictions critical for a symbiotic lifestyle and verify their active expression within the host
218 community.

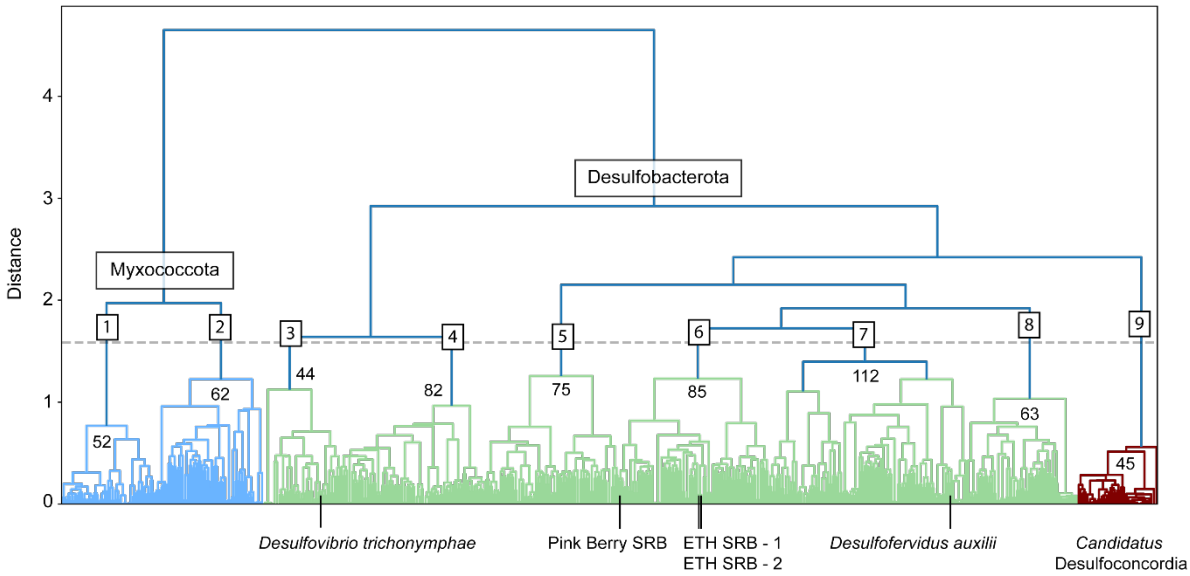

Figure 3: "*Ca.* Desulfoconcordia" are functionally distinct from other syntrophic Desulfobacteria based on comparative protein domain content Protein content similarity in a dendrogram built using the MEBS tool including 620 genomes, 45 of which are "*Ca.* Desulfoconcordia." All genomes were mapped against an existing set of Pfam domains and clustered based on their presence or absence using Jaccard distance and Ward variance minimization. The number of genomes present in each cluster is indicated within each cluster. Sulfate-reducing bacteria engaged in syntrophic or symbiotic relationships were marked in their respective clusters.

To look beyond general COG20-assigned functional annotations, we generated a comparative profile of over 19,000 documented functional protein domains and families present in the PfamV34 database. To do this, we compared the 46 symbiont genomes to a large existing set of 575 NCBI genomes representing the sulfate-reducing phyla Desulfobacterota and Myxococcota and used the Multigenomic Entropy Based Score (MEBS) workflow (De Anda et al., 2017; Langwig et al., 2022). Using a presence/absence clustering approach on these functional domain annotations, we observed that "*Ca.* Desulfoconcordia" endosymbionts form a separate cluster (cluster 9) different to the clusters for other members of the Desulfobacteria class (clusters 6, 7, and 8) and other SRB engaged in syntrophic or symbiotic relationships (in clusters 3, 6, and 7) (**Fig. 3**). Our analysis identified functional protein domains unique to the endosymbiont cluster compared to other Desulfobacteria clusters, including peptidases, an ATP/ADP transporter, viral components, and domains of unknown function. (**Table S6**). A few examples of functional domains present in 70% of genomes in the Desulfobacteria-

240 containing clusters (cluster 6, 7, and 8; **Fig. 3**) and absent in 100% of the symbiont genomes
241 include the CutA1 divalent ion tolerance protein (cluster 6), Ppx/GppA phosphatase family
242 (cluster 7), and PTS systems for sorbose/mannose uptake (cluster 8).

243 **Illustrating the core metabolism of the "*Ca.* Desulfoconcordia" symbiont**

244 We next build an overview of the metabolism of "*Ca.* Desulfoconcordia" symbionts, including
245 gene expression in the symbiotic consortium of one Mediterranean host species, *Olavius*
246 *algarvensis* (**Fig. 2a**). To gain a comprehensive view of the symbionts' expressed metabolism,
247 we combined mass spectrometric analysis of symbiont-enriched metaproteomes with
248 reanalyzed protein expression data from individual hosts, using an updated protein annotation
249 database (See **Methods** for data accession). The metaproteomes generated from the density-
250 separated fraction of homogenates from 50 worm hosts allowed us to target low-abundance
251 symbiont proteins, whereas single worm re-analyses allowed us to look into the top expressed
252 proteins for individual symbiont communities from *in situ* collected hosts. These
253 complementary analyses provide a comprehensive understanding of "*Ca.* Desulfoconcordia"
254 in *Olavius algarvensis* and a more detailed view of the variations in gene expression at the
255 individual community level (**Fig. S4**).

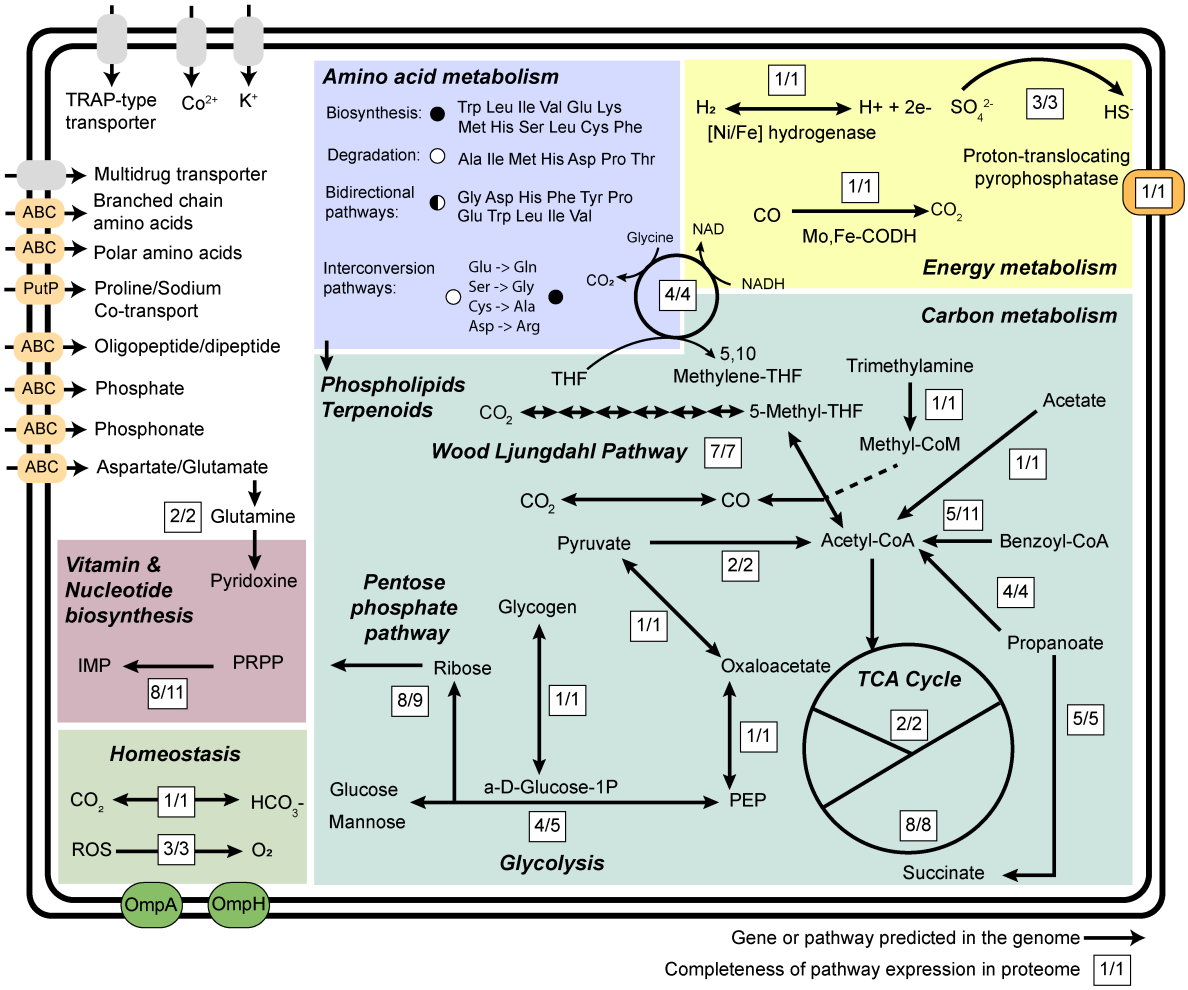

Figure 4: Expressed metabolism of "*Ca.* Desulfoconcordia" in the host *Olavius algarvensis*. The presence of a pathway or individual proteins (arrows) indicates the detection of proteins or pathways in the metaproteome. In instances where one or more genes from the pathway were not detected in the proteome, we indicated a fraction of pathway completeness in a rectangle. Amino acids are listed in different metabolic categories if at least one marker gene related to the metabolism of that AA is present in the expression data. The directionality of the amino acid metabolic pathway in which each AA is a part is indicated with black and white circles (black: biosynthetic, white: degradation, black/white: bidirectional pathways).

Our joint genome and proteome analysis confirmed that "*Ca.* Desulfoconcordia" in *Olavius algarvenisis* sulfate as a terminal electron acceptor via the dissimilatory sulfate reduction pathway and oxidize acetate to CO_2 (**Fig 4, Fig. S3, Table S5**). The methyl and carbonyl branches of the Wood-Ljungdahl pathway were completely expressed, indicating their capacity to oxidize acetate to CO_2. The symbionts expressed both the complete TCA cycle including the conversion of isocitrate to alpha-ketoglutarate, succinyl-CoA, and succinate, a pathway that

271 generates energy and releases two molecules of CO_2 and the glyoxylate bypass of the complete
272 TCA cycle. The glyoxylate pathway bypasses production of CO_2 molecules, ultimately
273 conserving carbon atoms during the degradation of two-carbon compounds (Ahn et al., 2016).
274 The symbionts also expressed the glycine cleavage pathway, which catabolizes glycine,
275 donates a methylene group to tetrahydrofolate, produces NADH that can be used for energy
276 generation, and generates ammonia as a nitrogen source in the complete ammonium
277 assimilation pathways. Unlike organisms that are limited to obligate anaerobic or obligate
278 aerobic carbon monoxide dehydrogenase activity, Ca. Desulfoconcoria expressed both the
279 anaerobic bifunctional carbon monoxide dehydrogenase found in the Wood-Ljungdahl
280 pathway (Nickel-cofactor-CODH; EC 1.2.7.4) and the oxygen-tolerant unidirectional carbon
281 monoxide dehydrogenase (Mo,Fe-CODH; CoxM EC 1.2.5.3) for the conversion of CO to CO_2.

282 Analysis of the metaproteome data from single-host individuals (n=10, **Fig. S4**) allowed us to
283 confirm the top expressed genes and identify potential individual community variability. In all
284 instances, the most highly expressed gene was annotated as a hypothetical protein, exhibiting
285 approximately 50% sequence identity (e-value of 10^{-109}) with porin family proteins from
286 members of the Desulfobacterota phylum in the NCBI BLAST database. Among the top 10
287 expressed genes were ABC transporters for amino acids and GroEL, a chaperone protein.
288 Additionally, the anaerobic bidirectional form of carbon monoxide dehydrogenase consistently
289 falls within the top 100 expressed genes from single-host individuals. Overall, this individual
290 host community analysis was congruent with the bulk analysis and revealed only minor
291 variations in "*Ca.* Desulfoconcordia" expressed metabolism between host individuals (**Fig.
292 S4**).

Discussion & Conclusions

Sulfate reducing bacteria are found in a wide range of habitats and have been shown to engage in both syntrophic associations with other bacteria and cross-domain symbiotic relationships (Barton & Fauque, 2022). By broadening the scope to encompass the entire phylum of Desulfobacterota, we can gain insights into the extensive associations of these bacteria, all of which fall under the overarching metabolic guild of 'dissimilatory sulfate-reducers.' For instance, sulfate-reducing *Desulfofustis* form free-living aggregates with purple sulfur bacteria, forming what is known as the "pink berry" consortia (Wilbanks et al., 2014). Various species of *Desulfovibrio* establish symbiotic relationships with sea cucumbers, cockchafer larvae, and termites, as well as with the gut fauna of numerous mammalian species (Barton & Fauque, 2022). The sulfate-reducing bacteria described here are unique in that they present a model for studying the co-occurrence of a syntrophic interaction with sulfur-reliant bacteria (Dubilier et al., 2001) and the provisioning of metabolic capabilities to multiple genera of an animal host family across the oceans (Kleiner et al., 2012; Mankowski et al., 2021; Ruehland et al., 2008).

To determine whether the metabolism of these symbionts could be correlated with that of their close relatives, we placed them in their taxonomic context among the available Genome Taxonomy Database (GTDB) genera. The closest phylogenetic relatives of *Candidatus* Desulfoconcordia included uncultivated environmental genomes representing five genera (as defined by the Genome Taxonomy Database). They fall within a well-supported branch of the Desulfobacteria class, which includes functionally characterized cultivars (e.g., *Desulfonema, Desulfococcus, Desulfatitalea,* and *Desulfosarcina*). Two such closely related SRB cultivars, *Dn. magnum* and *Dn. limicola,* represent a diverse set of metabolic capabilities that are not ubiquitous to their respective clade. These cultivars were recently profiled using proteogenomic techniques (Schnaars et al., 2021). Although they were shown to share the capacity for short-chain fatty acid degradation they also had clear differences in core metabolic

318 functions. *Dn. magnum* uniquely encoded malate, benzoate, p-cresol, and 4-hydroxybenzoate
319 degradation, whereas *Dn. limicola* species were unable to grow on complex aromatic
320 compounds, but did have the capacity to grow chemolithoautotrophically on H_2 and CO_2 as
321 energy and carbon sources (Schnaars et al., 2021). Considering the metabolic variability even
322 within a genus, the placement of "*Ca.* Desulfoconcordia" symbionts in a phylogenetic context
323 in relation to other sulfate-reducers only allows us to hypothesize about their general core
324 metabolism. Within the phylum Desulfobacterota, phylogenetic relationships alone are not
325 sufficient to infer specific metabolic functions as seen in the above examples and the "*Ca.*
326 Desulfoconcordia" symbionts.

327 Recently, metagenomes of the newly reclassified phyla Desulfobacterota, SAR324, and
328 Myxococcota were compiled and a protein-functional-domain-based clustering analysis was
329 performed to add context to our general understanding of the metabolic capabilities of what
330 were previously referred to as Deltaproteobacteria (Langwig et al., 2022). Many of the broad
331 metabolic clusters in the Myxococcota and Desulfobacterota phyla were consistent in their
332 phylogeny except for two clusters, which were defined as cluster D and F (here clusters 6 and
333 7, see **Fig. 3**) that encompassed the class Desulfobacteria. This pattern led us to hypothesize
334 that the "*Ca.* Desulfoconcordia" symbionts, which belong to the Desulfobacteria class, would
335 fall into one of these two clusters based on their genome size, sulfate reduction capacity, and
336 completeness of their acetate oxidation pathways. However, in performing the extended
337 analysis with the MEBS pipeline, we observed that the "*Ca.* Desulfoconcordia" endosymbiont
338 genomes form a distinct metabolic cluster with respect to the previously defined clusters. This
339 "*Ca.* Desulfoconcordia" cluster differs from other Desulfobacteria clusters in the presence of
340 peptidases, transport ion channel proteins, and multiple domains of unknown function and the
341 absence of certain stress response genes (PPX/GppA system) and sugar uptake.

342 This study presented "*Ca.* Desulfoconcordia" gene annotations, functional enrichment
343 comparisons of symbiont genomes vs. their closest genus-level relatives, and the
344 metaproteomics fingerprint of one representative symbiont. We found that "*Ca.*
345 Desulfoconcordia" encoded for and expressed a variety of metabolic capabilities including the
346 import of amino acids, peptides, and carbohydrates, and central heterotrophic catabolic cycles.
347 The diversity of ABC transporters for amino acids points to a potential energy-saving
348 mechanism for these symbiotic heterotrophs, as hypothesized in a previous study (Kleiner et
349 al., 2012). In a system where these cells are closely associated with neighboring bacteria and
350 host cells, these organisms could utilize this mechanism of scavenging free amino acids for
351 either building blocks or a nitrogen source. In contrast, the genes for sulfonate transport
352 (TauABCD system) were enriched in the majority of free-living genomes and absent in all
353 symbiont genomes. This TauABCD gene cluster was originally described in *E. coli* and confers
354 the ability to use aliphatic sulfonates as a sulfur source for growth when free sulfate is limited
355 or absent (Javaux et al., 2007). The "*Ca.* Desulfoconcordia" symbionts provide reduced sulfidic
356 compounds to their neighboring chemoautotrophic partners and they also have access to sulfate
357 from both the external sediment and sulfate released from the sulfur oxidation of these partner
358 bacteria (Dubilier et al., 2001; Kleiner et al., 2012; Ruehland et al., 2008; Woyke et al., 2006).
359 This abundance of their main terminal electron acceptors from multiple sources within their
360 habitat can explain the lack of sulfur-scavenging genes.

361 *"Ca.* Desulfoconcordia" symbionts express both the anaerobic bidirectional carbon monoxide
362 dehydrogenase (EC 1.2.7.4), which is crucial for the functioning of the Wood-Ljungdahl
363 pathway, and the aero-tolerant unidirectional carbon monoxide dehydrogenase (EC 1.2.5.3),
364 which oxidizes carbon monoxide to CO_2 and H_2 as a source of energy for the organism (Ritacca
365 et al., 2022). In a recent study, a facultative anaerobic Bacillota cultivar was shown to encode
366 the same two versions of CODH and was able to alternate the use of either enzyme depending

367 on oxygen and nitrate concentrations (Imaura et al., 2023). The host worms of the "*Ca.*
368 Desulfoconcordia" symbionts travel between anoxic and oxic sediment layers along a typical
369 stratified gradient of electron acceptors, which facilitates the co-occurrence of aero-tolerant
370 and anaerobic symbionts in one host (Dubilier et al., 2001; Kleiner et al., 2012; Woyke et al.,
371 2006). These environmental conditions induced by host movement could be the reason why
372 the "*Ca.* Desulfoconcordia" symbionts have both an anaerobic and aerotolerant form of the
373 CODH enzyme. The 4Fe-4S cluster of the Wood-Ljungdahl pathway CODH would be highly
374 sensitive (Ragsdale et al., 1983) in an oxic habitat, preventing the oxidation of acetyl-CoA.
375 During this phase, the aerotolerant CODH could continue to remove CO, which is present
376 either as a byproduct of sulfate reduction or as an environmental input from the surrounding
377 pore water (Kleiner et al., 2015). This mechanism can maintain cellular reducing equivalents
378 under oxygen stress until the cells are once again under anaerobic conditions. Sulfate-reducing
379 bacteria are often found in anoxic conditions but can also be facultative aerobes in response to
380 oxic conditions (Hao et al., 1996; Muyzer & Stams, 2008; Teske et al., 1998). Adaptability to
381 quickly changing redox conditions would be an advantage in this specific symbiotic lifestyle
382 (Woyke et al., 2006). Whereas in free-living ecosystems or other symbioses, sulfate-reducers
383 are more likely to physically stratify according to their oxygen requirements as in vertically
384 stratified microbial mats or the radial oxic-anoxic compartmentalization inside termite guts
385 (Brune & Friedrich, 2000; Casillas-Martínez et al., 2005; Dyer, 2004; Stolz, 2000).

386 The results of this proteogenomic study reiterated prior observations that the phylogeny of
387 sulfate-reducing bacteria does not always correlate directly with their extended metabolic
388 functions (Langwig et al., 2022). Our results suggested that specific metabolic capabilities were
389 unique to "*Ca.* Desulfoconcordia" SRB symbionts when compared with free-living SRBs,
390 cultivars, and other syntrophic Desulfobacteria (e.g. the presence of certain peptidases, amino
391 acid-binding proteins, and outer membrane transporters in the symbiotic lifestyle). The "*Ca.*

392 Desulfoconcordia" symbiont of the host species *Olavius algarvensis* expressed many of the
393 expected core metabolic pathways of Desulfobacteria – with high representation of two types
394 of carbon monoxide dehydrogenase and amino acid importers. Our proteogenomic approach
395 allowed us to uncover the expression of genes at the protein level, which ultimately
396 demonstrated which metabolic pathways were truly environmentally relevant for these
397 organisms. While core metabolic pathways like carbon monoxide oxidation and amino acid
398 import are consistent with Desulfobacteria, many distinguishing protein domains remain
399 uncharacterized. Approximately 50% of the most abundant proteins are hypothetical,
400 underscoring the need for future studies combining proteomics with protein modeling to
401 uncover the active but unknown metabolism of "*Ca.* Desulfoconcordia" and their roles in
402 symbiosis.

403 **Methods**

404 **Sample collection**

405 The metagenome-assembled genome bins of "*Ca.* Desulfoconcordia" from different host
406 species from various field sites were generated in a previous study (Mankowski et al., 2021).
407 These genomes served as the basis for all metagenomic analyses in this study.

408 *Olavius algarvensis* worms for the density centrifugation metaproteomes were collected from
409 the Sant'andrea Bay on the island of Elba, Italy (7 m depth; 42°48'31.13"N, 10° 8'31.28"E) in
410 September of 2020. The animals were collected from the sediment by decantation with
411 seawater and identified using both a dissection scope and fluorescence microscope. The density
412 centrifugation protocol was carried out in the field and the samples were transported and stored
413 at -80 C prior to protein extraction and digestion.

414

415 **Phylogenomic analyses**

416 Two trees were constructed to provide 1) a broad overview of the Desulfobacterota phylum
417 that was used in downstream protein functional domain analysis (Fig. 1a) and Fig. 2) a more
418 specific look at the phylogenetic placement of the symbiont genomes in the Desulfobacteria
419 class (Fig. 1b). For the construction of the first tree, a set of previously curated genomes from
420 NCBI (Langwig et al., 2022) representing the Desulfobacterota and Myxococcota phyla were
421 downloaded and dereplicated along with symbiont genomes with dRep (-pa 0.9 -sa 0.95 -comp
422 70 -con 50). The phylogenomic software iqtree2 was used to build a maximum likelihood tree
423 (-m TEST -B 10000 --alrt 10000 -T AUTO) and the best fit model was determined to be
424 LG+I+G4. To construct of the second tree and to determine the most well-supported outgroup
425 based on all available sequences (rather than a pre-curated dataset), the GToTree workflow for
426 building a phylogenomic tree with all available Genome Taxonomy Database (GTDB)
427 reference sequences was used (Lee, 2019, https://github.com/AstrobioMike/GToTree). This
428 second tree was constructed with the available GTDB sequences in the Desulfobacteria class
429 with Syntrophobacteria and Desulfobaccia as outgroups. GToTree automatically identifies
430 single-copy genes (SCGs) based on pre-curated hidden Markov model (HMM) gene sets, aligns
431 with Muscle, trims with Trimal, builds a FastTree and can be piped directly into iqtree2
432 (https://github.com/AstrobioMike/GToTree/wiki/example-usage). The pre-curated Bacteria
433 HMM set containing 76 gene targets was chosen to generate these trees. The FastTree step was
434 followed by iqtree2 (-m TEST -B 10000 --alrt 10000 -T AUTO) with the best model fit
435 determined to be Q.yeast+I+G4. The resulting trees were uploaded to iTol for visual annotation
436 (Letunic & Bork, 2016) of taxonomy for the overlaying additional analyses.

437 **Pangenome Analysis**

438 Anvi'o (v7.1) (Eren et al., 2021) was used to construct a pangenome that compares "*Ca*.
439 Desulfoconcordia" symbionts to the other members of the well-supported (>95% bootstrap)

440 GTDB free-living clade in which the symbiont genomes fall. The standard workflow for
441 constructing a pangenome was followed (https://merenlab.org/2016/11/08/pangenomics-v2/).
442 The contig databases were populated using all available hmm sources, kegg module
443 annotations, single-copy core gene taxonomy, tRNA scan, and the NCBI COG20 database
444 (anvi-run-hmms, anvi-run-scg-taxonomy, anvi-scan-trnas, anvi-run-ncbi-cogs, and anvi-run-
445 kegg-kofams). Functional enrichment analyses were performed between the "free-living" and
446 "symbiotic" categories on bothkegg module completeness and COG20 functional annotations.

447 **Metabolic Annotation and Profiling**

448 The MEBS software tool (De Anda et al., 2017) was used to further investigate and compare
449 the metabolic capabilities of the assembled symbiont MAGs with respect to the reference
450 genomes used in the first phylogenomic tree. The Prodigal gene predictions from the checkM
451 output (generated by the dRep step described above) were used as the input for the MEBS
452 scoring pipeline. Protein clustering was performed by first annotating the genomes against the
453 most recently available Pfam database release (PfamV34) and then using the mebs_clust.py
454 script to hierarchically cluster using Jaccard distance, Ward variance minimization, and a
455 maximum distance threshold of 0.3. In accordance with previous analyses (Langwig et al.,
456 2022), cluster distances were tested at 0.3, 0.35, 0.4, and 0.5 and 0.35 was chosen as the
457 clustering of the different classes in the Desulfobacterota and Myxococcota phyla closely
458 resembled the result published in the initial study.

459

460 **Metaproteomic analyses:**

461 **Reanalysis of published data**

462 Publically available metaproteomic data were downloaded from the PRIDE
463 (https://www.ebi.ac.uk/pride/) repository for reanalysis (Project ID: PXD014591). These mass
464 spectrometry files were searched in Proteome Discoverer 2.5 against an updated
465 metaproteomic reference database (OlaviusV13.fasta). The MS/MS spectra were searched
466 against this reference database using the Sequest HT algorithm in Proteome Discoverer 2.5
467 (Thermo Fisher Scientific) with the following parameters: trypsin (full), maximum of two
468 missed cleavages, 10 pp precursor mass tolerance, 0.1-Da fragment mass tolerance, and a
469 maximum of three dynamic modifications per peptide. False discovery rates (FDRs) for peptide
470 spectral matches (PSMs) were calculated and filtered using the Percolator node in the Proteome
471 Discoverer. The Protein FDR Validator node was used to calculate q values for proteins based
472 on the false discovery rates calculated by searching against the target-decoy database. Proteins
473 with q values of < 0.01 were categorized as high-confidence and those with q-values between
474 0.01 – 0.05 were categorized as medium-confidence. We combined all search results into a
475 multiconsensus report and proteins were filtered to retain only those with an overall FDR of
476 5% or less. Normalized spectral abundance factors (NSAFs) were calculated for each bacterial
477 and animal species (OrgNSAF) and multiplied by 100 to represent relative protein abundance
478 as a percentage.

479 **Density centrifugation, protein extraction, and 2D-LC-MS/MS for the generation of**
480 **deep metaproteomes**

481 Single *Olavius algarvensis* worms were pooled (n=50), homogenized, and density centrifuged
482 according to the protocol published by Kleiner et al. (2012). Tryptic peptides were prepared
483 using the filter-aided sample preparation method (FASP), adapted from a previously published
484 method (Wiśniewski et al., 2009). Proteins were digested into peptides using Pierce MS-grade

485 trypsin (Thermo Fischer Scientific) and the resulting peptides were quantified using the Pierce
486 micro-bicinchoninic acid (BCA) kit (Thermo Fisher Scientific), following the manufacturer
487 instructions.
488 To generate metaproteomes with the best possible coverage of low abundant peptides, the
489 peptides were analyzed with an on-line 2D-LC-MS/MS method using an Ultimate3000
490 RSLCnano system (Thermo Fisher Scientific). Samples were loaded onto a strong cation
491 exchange (SCX) reverse-phase column (Thermo Fisher Scientific). The downstream C18
492 Acclaim PepMap 100 pre-column was first placed in-line with the Easy-Spray PepMap C18
493 analytical column (75um by 75cm; Thermo Fisher Scientific) and peptides were separated with
494 a gradient of eluent A (100% uHPLC water + 0.1% formic acid) and eluent B (20/80 uHPLC
495 water/acetonitrile + 0.1% formic acid). After this first wash, peptides were eluted from the SCX
496 column to the C18 pre-column and subsequently to the C18 analytical column with salt plugs
497 along a gradually increasing pH gradient (pH: 2.5, 3, 3.5, 4. 4.5, 5, 5.5, 6, 7, 8). Eluting peptides
498 were ionized with electrospray ionization and analyzed using data-dependent acquisition in a
499 Q-Exactive Orbitrap mass analyzer (Thermo Fisher Scientific). Resulting mass spectrometry
500 files were uploaded to Proteome Discoverer 2.5 and searched with the same parameters and
501 filters described above for the reanalysis of published datasets.

502

503 **Author contributions:**

504 GD, ML, and ND conceived the study. GD collected metagenomic data and performed
505 phylogenomic, metabolic annotations, and pangenome analyses. AM generated the "*Ca*.
506 Desulfoconcordia" metagenome-assembled genome bins. JCA and VDA provided input on the
507 phylogenomics and MEBS analyses respectively. GD, MV, and MK generated mass
508 spectrometry data and performed metaproteome analyses. GD, ML and EK wrote the
509 manuscript with contributions from ND, MK, AM, MV, JCA, and VDA.

510 **Acknowledgements**

511 We thank Silke Wetzel (Max Planck Institute for Marine Microbiology) for help with
512 laboratory work for this project. We thank Miriam Weber and Christian Lott (HYDRA Marine
513 Sciences GmbH) for their support collecting samples in the field and Olivier Lemaire (Max
514 Planck Institute for Marine Microbiology) for helpful discussions. All LC-MS/MS
515 measurements were made in the Molecular Education, Technology, and Research Innovation
516 Center (METRIC) at North Carolina State University. This study was funded by the Max
517 Planck Society, the Gottfried Wilhelm Leibniz-Prize of the German Research Foundation
518 (DFG) to Nicole Dubilier, and the US National Science Foundation (grant IOS #2426305 to
519 Manuel Kleiner).

520 **Data availability**

521 The sequencing data for this study will be deposited to the European Nucleotide Archive
522 (ENA) at EMBL-EBI upon review and are available upon request. Proteomics data that were
523 reanalyzed are available in the PRIDE repository under the Project ID: PXD014591 and
524 proteomics data generated for this study will be made available upon request.

525

Ahn, S., Jung, J., Jang, I.-A., Madsen, E. L., & Park, W. (2016). Role of glyoxylate shunt in oxidative stress response. *The Journal of Biological Chemistry*, *291*(22), 11928–11938. https://doi.org/10.1074/jbc.M115.708149

Barton, L. L., & Fauque, G. D. (2022). Interactions of SRB with animals and plants. In L. L. Barton & G. D. Fauque (Eds.), *Sulfate-Reducing Bacteria and Archaea* (pp. 529–554). Springer International Publishing. https://doi.org/10.1007/978-3-030-96703-1_10

Bergin, C., Wentrup, C., Brewig, N., Blazejak, A., Erséus, C., Giere, O., Schmid, M., De Wit, P., & Dubilier, N. (2018). Acquisition of a novel sulfur-oxidizing symbiont in the gutless marine worm *Inanidrilus exumae*. *Applied and Environmental Microbiology*, *84*(7), e02267-17. https://doi.org/10.1128/AEM.02267-17

Brune, A., & Friedrich, M. (2000). Microecology of the termite gut: Structure and function on a microscale. *Current Opinion in Microbiology*, *3*(3), 263–269. https://doi.org/10.1016/S1369-5274(00)00087-4

Casillas-Martínez, L., Gonzalez, M., Fuentes, Z., Castro, C., Nieves-Mendez, D., Hernandez, C., Ramirez, W., Sytsma, R., Perez-Jimenez, J. R., & Visscher, P. (2005). Community structure, geochemical characteristics and mineralogy of a hypersaline microbial mat, Cabo Rojo, PR. *Geomicrobiology Journal*, *22*, 269–281. https://doi.org/10.1080/01490450500182672

De Anda, V., Zapata-Peñasco, I., Eguiarte, L. E., & Souza, V. (2018). The sulfur cycle as the gear of the "Clock of Life": The point of convergence between geological and genomic data in the Cuatro Cienegas basin. In F. García-Oliva, J. Elser, & V. Souza (Eds.), *Ecosystem Ecology and Geochemistry of Cuatro Cienegas: How to Survive in an Extremely Oligotrophic Site* (pp. 67–83). Springer International Publishing. https://doi.org/10.1007/978-3-319-95855-2_6

De Anda, V., Zapata-Peñasco, I., Poot-Hernandez, A. C., Eguiarte, L. E., Contreras-Moreira, B., & Souza, V. (2017). MEBS, a software platform to evaluate large (meta)genomic collections according to their metabolic machinery: Unraveling the sulfur cycle. *GigaScience*, *6*(11), gix096. https://doi.org/10.1093/gigascience/gix096

Diao, M., Dyksma, S., Koeksoy, E., Ngugi, D. K., Anantharaman, K., Loy, A., & Pester, M. (2023). Global diversity and inferred ecophysiology of microorganisms with the potential for dissimilatory sulfate/sulfite reduction. *FEMS Microbiology Reviews*, *47*(5), fuad058. https://doi.org/10.1093/femsre/fuad058

Dombrowski, N., Teske, A. P., & Baker, B. J. (2018). Expansive microbial metabolic versatility and biodiversity in dynamic Guaymas Basin hydrothermal sediments. *Nature Communications*, *9*(1), 4999. https://doi.org/10.1038/s41467-018-07418-0

Dubilier, N., Mülders, C., Ferdelman, T., de Beer, D., Pernthaler, A., Klein, M., Wagner, M., Erséus, C., Thiermann, F., Krieger, J., Giere, O., & Amann, R. (2001). Endosymbiotic sulphate-reducing and sulphide-oxidizing bacteria in an oligochaete worm. *Nature*, *411*(6835), 298–302. https://doi.org/10.1038/35077067

Dyer, B. D. (2004). Termite hindgut symbionts. In J. Seckbach (Ed.), *Symbiosis* (Vol. 4, pp. 701–713). Kluwer Academic Publishers. https://doi.org/10.1007/0-306-48173-1_44

Eren, A. M., Kiefl, E., Shaiber, A., Veseli, I., Miller, S. E., Schechter, M. S., Fink, I., Pan, J. N., Yousef, M., Fogarty, E. C., Trigodet, F., Watson, A. R., Esen, Ö. C., Moore, R. M., Clayssen, Q., Lee, M. D., Kivenson, V., Graham, E. D., Merrill, B. D., … Willis, A. D. (2021). Community-led, integrated, reproducible multi-omics with anvi'o. *Nature Microbiology*, *6*(1), 3–6. https://doi.org/10.1038/s41564-020-00834-3

Giere, O., & Erséus, C. (2002). Taxonomy and new bacterial symbioses of gutless marine Tubificidae (Annelida, Oligochaeta) from the Island of Elba (Italy). *Organisms Diversity & Evolution*, *2*(4), 289–297. https://doi.org/10.1078/1439-6092-00044

Goris, J., Konstantinidis, K. T., Klappenbach, J. A., Coenye, T., Vandamme, P., & Tiedje, J. M. (2007). DNA–DNA hybridization values and their relationship to whole-genome sequence similarities. *International Journal of Systematic and Evolutionary Microbiology*, *57*(1), 81–91. https://doi.org/10.1099/ijs.0.64483-0

Hao, O. J., Chen, J. M., Huang, L., & Buglass, R. L. (1996). Sulfate-reducing bacteria. *Critical Reviews in Environmental Science and Technology*, *26*(2), 155–187. https://doi.org/10.1080/10643389609388489

Imaura, Y., Okamoto, S., Hino, T., Ogami, Y., Katayama, Y. A., Tanimura, A., Inoue, M., Kamikawa, R., Yoshida, T., & Sako, Y. (2023). Isolation, genomic sequence and physiological characterization of *Parageobacillus* sp. G301, an isolate capable of both hydrogenogenic and aerobic carbon monoxide oxidation. *Applied and Environmental Microbiology*, *89*(6), e00185-23. https://doi.org/10.1128/aem.00185-23

Javaux, C., Joris, B., & De Witte, P. (2007). Functional characteristics of TauA binding protein from TauABC *Escherichia coli* system. *The Protein Journal*, *26*(4), 231–238. https://doi.org/10.1007/s10930-006-9064-x

Kleiner, M., Polerecky, L., Lott, C., Bergin, C., Häusler, S., Liebeke, M., Wentrup, C., Musat, N., Kuypers, M. M. M., & Dubilier, N. (2023). *Mechanism of high energy efficiency of carbon fixation by sulfur-oxidizing symbionts revealed by single-cell analyses and metabolic modeling* (p. 2023.11.25.568684). bioRxiv. https://doi.org/10.1101/2023.11.25.568684

Kleiner, M., Wentrup, C., Holler, T., Lavik, G., Harder, J., Lott, C., Littmann, S., Kuypers, M. M. M., & Dubilier, N. (2015). Use of carbon monoxide and hydrogen by a bacteria-animal symbiosis from seagrass sediments. *Environmental Microbiology*, *17*(12), 5023–5035. https://doi.org/10.1111/1462-2920.12912

Kleiner, M., Wentrup, C., Lott, C., Teeling, H., Wetzel, S., Young, J., Chang, Y.-J., Shah, M., VerBerkmoes, N. C., Zarzycki, J., Fuchs, G., Markert, S., Hempel, K., Voigt, B., Becher, D., Liebeke, M., Lalk, M., Albrecht, D., Hecker, M., … Dubilier, N. (2012). Metaproteomics of a gutless marine worm and its symbiotic microbial community reveal unusual pathways for carbon and energy use. *Proceedings of the National Academy of Sciences*, *109*(19), E1173–E1182. https://doi.org/10.1073/pnas.1121198109

Kushkevych, I., Cejnar, J., Treml, J., Dordević, D., Kollar, P., & Vítězová, M. (2020). Recent advances in metabolic pathways of sulfate reduction in intestinal bacteria. *Cells*, *9*(3), 698. https://doi.org/10.3390/cells9030698

Langwig, M. V., De Anda, V., Dombrowski, N., Seitz, K. W., Rambo, I. M., Greening, C., Teske, A. P., & Baker, B. J. (2022). Large-scale protein level comparison of Deltaproteobacteria reveals cohesive metabolic groups. *The ISME Journal*, *16*(1), 307–320. https://doi.org/10.1038/s41396-021-01057-y

Lee, M. D. (2019). GToTree: A user-friendly workflow for phylogenomics. *Bioinformatics*, *35*(20), 4162–4164. https://doi.org/10.1093/bioinformatics/btz188

Letunic, I., & Bork, P. (2016). Interactive tree of life (iTOL) v3: An online tool for the display and annotation of phylogenetic and other trees. *Nucleic Acids Research*, *44*(W1), W242-245. https://doi.org/10.1093/nar/gkw290

Mankowski, A., Kleiner, M., Erséus, C., Leisch, N., Sato, Y., Volland, J.-M., Hüttel, B., Wentrup, C., Woyke, T., Wippler, J., Dubilier, N., & Gruber-Vodicka, H. (2021). Highly variable fidelity drives symbiont community composition in an obligate symbiosis. *BioRxiv*. https://doi.org/10.1101/2021.04.28.441735

Muyzer, G., & Stams, A. J. M. (2008). The ecology and biotechnology of sulphate-reducing bacteria. *Nature Reviews Microbiology*, *6*(6), 441–454. https://doi.org/10.1038/nrmicro1892

Postgate, J. R. (1979). *The sulphate-reducing bacteria*. CUP Archive.

Ragsdale, S. W., Clark, J. E., Ljungdahl, L. G., Lundie, L. L., & Drake, H. L. (1983). Properties of purified carbon monoxide dehydrogenase from *Clostridium thermoaceticum*, a nickel, iron-sulfur protein. *Journal of Biological Chemistry*, *258*(4), 2364–2369. https://doi.org/10.1016/S0021-9258(18)32932-6

Ritacca, A. G., Rovaletti, A., Moro, G., Cosentino, U., Ryde, U., Sicilia, E., & Greco, C. (2022). Unraveling the reaction mechanism of Mo/Cu CO dehydrogenase using QM/MM calculations. *ACS Catalysis*, *12*(12), 7336–7343. https://doi.org/10.1021/acscatal.2c01408

Ruehland, C., Blazejak, A., Lott, C., Loy, A., Erséus, C., & Dubilier, N. (2008). Multiple bacterial symbionts in two species of co-occurring gutless oligochaete worms from Mediterranean sea grass sediments. *Environmental Microbiology*, *10*(12), 3404–3416. https://doi.org/10.1111/j.1462-2920.2008.01728.x

Sato, Y., Wippler, J., Wentrup, C., Ansorge, R., Sadowski, M., Gruber-Vodicka, H., Dubilier, N., & Kleiner, M. (2022). Fidelity varies in the symbiosis between a gutless marine worm and its microbial consortium. *Microbiome*, *10*(178), 1–18. https://doi.org/10.1186/s40168-022-01372-2

Schnaars, V., Wöhlbrand, L., Scheve, S., Hinrichs, C., Reinhardt, R., & Rabus, R. (2021). Proteogenomic insights into the physiology of marine, sulfate-reducing, filamentous *Desulfonema limicola* and *Desulfonema magnum*. *Microbial Physiology*, *31*(1), 36–56. https://doi.org/10.1159/000513383

Stolz, J. F. (2000). Structure of microbial mats and biofilms. In R. E. Riding & S. M. Awramik (Eds.), *Microbial Sediments* (pp. 1–8). Springer. https://doi.org/10.1007/978-3-662-04036-2_1

Tee, H. S., Waite, D., Lear, G., & Handley, K. M. (2021). Microbial river-to-sea continuum: Gradients in benthic and planktonic diversity, osmoregulation and nutrient cycling. *Microbiome*, *9*, 190. https://doi.org/10.1186/s40168-021-01145-3

Teske, A., Ramsing, N. B., Habicht, K., Fukui, M., Küver, J., Jørgensen, B. B., & Cohen, Y. (1998). Sulfate-Reducing Bacteria and Their Activities in Cyanobacterial Mats of Solar Lake (Sinai, Egypt). *Applied and Environmental Microbiology*, *64*(8), 2943–2951. https://www.ncbi.nlm.nih.gov/pmc/articles/PMC106797/

Wilbanks, E. G., Jaekel, U., Salman, V., Humphrey, P. T., Eisen, J. A., Facciotti, M. T., Buckley, D. H., Zinder, S. H., Druschel, G. K., Fike, D. A., & Orphan, V. J. (2014). Microscale sulfur cycling in the phototrophic pink berry consortia of the Sippewissett Salt Marsh. *Environmental Microbiology*, *16*(11), 3398–3415. https://doi.org/10.1111/1462-2920.12388

Wiśniewski, J. R., Zougman, A., Nagaraj, N., & Mann, M. (2009). Universal sample preparation method for proteome analysis. *Nature Methods*, *6*(5), 359–362. https://doi.org/10.1038/nmeth.1322

Woyke, T., Teeling, H., Ivanova, N. N., Huntemann, M., Richter, M., Gloeckner, F. O., Boffelli, D., Anderson, I. J., Barry, K. W., Shapiro, H. J., Szeto, E., Kyrpides, N. C., Mussmann, M., Amann, R., Bergin, C., Ruehland, C., Rubin, E. M., & Dubilier, N. (2006). Symbiosis insights through metagenomic analysis of a microbial consortium. *Nature*, *443*(7114), 950–955. https://doi.org/10.1038/nature05192

Zimmermann, J., Wentrup, C., Sadowski, M., Blazejak, A., Gruber-Vodicka, H. R., Kleiner, M., Ott, J. A., Cronholm, B., De Wit, P., Erséus, C., & Dubilier, N. (2016). Closely coupled evolutionary history of ecto- and endosymbionts from two distantly related animal phyla. *Molecular Ecology*, *25*(13), 3203–3223. https://doi.org/10.1111/mec.13554